Cancer Research

CYP27A1 Loss Dysregulates Cholesterol Homeostasis in Prostate Cancer

Mahmoud A. Alfaqih[1,2], Erik R. Nelson[2,3], Wen Liu[2], Rachid Safi[2], Jeffery S. Jasper[2], Everardo Macias[1,4], Joseph Geradts[5], J. Will Thompson[2,6], Laura G. Dubois[6], Michael R. Freeman[4], Ching-yi Chang[2], Jen-Tsan Chi[7], Donald P. McDonnell[2], and Stephen J. Freedland[4,8]

Abstract

In this study, we used a bioinformatic approach to identify genes whose expression is dysregulated in human prostate cancers. One of the most dramatically downregulated genes identified encodes CYP27A1, an enzyme involved in regulating cellular cholesterol homeostasis. Importantly, lower CYP27A1 transcript levels were associated with shorter disease-free survival and higher tumor grade. Loss of CYP27A1 in prostate cancer was confirmed at the protein level by immunostaining for CYP27A1 in annotated tissue microarrays. Restoration of CYP27A1 expression in cells where its gene was silenced attenuated their growth in vitro and in tumor xenografts. Studies performed in vitro revealed that treatment of prostate cancer cells with 27-hydroxycholesterol (27HC), an enzymatic product of CYP27A1, reduced cellular cholesterol content in prostate cancer cell lines by inhibiting the activation of sterol regulatory-element binding protein 2 and downregulating low-density lipoprotein receptor expression. Our findings suggest that CYP27A1 is a critical cellular cholesterol sensor in prostate cells and that dysregulation of the CYP27A1/27HC axis contributes significantly to prostate cancer pathogenesis. Cancer Res; 1–12. ©2017 AACR.

Introduction

Prostate cancer is the most common non–skin cancer among men and the second leading cause of cancer death (1). Although the underlying causes of prostate cancer remain unclear, multiple epidemiologic studies have suggested that hypercholesterolemia is associated with an increased risk of high-grade metastatic disease (2–6). Indeed, prostate cancer cells and those of other solid tumors have been shown to contain higher cholesterol levels than juxtaposed normal cells (7, 8). Thus, it is possible that increased cholesterol content affects prostate cancer growth by satisfying the need of proliferating cells for a key component of cell membranes. Another contemporary opinion is that increased cellular cholesterol within mitochondrial membranes renders cells resistant to many chemotherapeutics (9). It has also been suggested that cholesterol affects prostate cancer growth by serving as a precursor for the production of intratumoral androgens (10). It is not surprising, therefore, that inhibitors of HMG-CoA-reductase (HMGCR; statins), drugs that block cholesterol synthesis and reduce serum cholesterol and inhibit prostate cancer cell growth in vitro (11, 12), are associated with reduced prostate cancer progression following treatment with surgical prostatectomy (13) or brachytherapy (14) and have been shown in population studies to be associated with a lower risk of developing metastatic or fatal prostate cancer (15–18). Given these positive data, it is noteworthy that not all studies have linked hypercholesterolemia with higher prostate cancer risk (19). Likewise, the data on statins are not universally positive in terms of their association with prostate cancer risk and/or prostate cancer progression with several studies finding no such association or with increased risk (20–23). Importantly, hypercholesterolemia and statin use influence serum cholesterol levels. Whether these changes effect intratumoral cholesterol is not clear. As such, given the scientific plausibility that cholesterol promotes prostate cancer progression, albeit in the face of equivocal epidemiologic data, it is important to understand the molecular mechanisms used by prostate cancer cells to regulate intracellular cholesterol.

In humans, the regulation of cellular cholesterol homeostasis is achieved primarily through the coordinated activity of two classes of transcription factors: Sterol regulatory element-binding proteins (SREBP) and Liver X Receptors (LXR; refs. 24–26). LXRs can regulate cholesterol efflux by inducing the expression of mRNAs encoding the reverse cholesterol ATP-binding cassette (ABC) transporters ABCA1 and ABCG1 (27), whereas SREBPs promote endogenous cholesterol synthesis and uptake of extracellular

[1]Department of Surgery, Duke University, Durham, North Carolina. [2]Department of Pharmacology and Cancer Biology, Duke University, Durham, North Carolina. [3]Department of Molecular and Integrative Physiology, University of Illinois at Urbana-Champaign; and University of Illinois Cancer Center, Chicago, Illinois. [4]Department of Surgery and Samuel Oschin Comprehensive Cancer Institute, Cedars-Sinai Medical Center, Los Angeles, California. [5]Department of Pathology, Brigham and Women's Hospital, Boston, Massachusetts. [6]Department of Proteomics and Metabolomics Shared Resource, Duke University, Durham, North Carolina. [7]Department of Molecular Genetics and Microbiology, Duke University, Durham, North Carolina. [8]Surgery Section, Durham VA Medical Center, Durham, North Carolina.

Note: Supplementary data for this article are available at Cancer Research Online (http://cancerres.aacrjournals.org/).

Current address for M.A. Alfaqih: Department of Physiology and Biochemistry, Jordan University of Science and Technology, Irbid, Jordan.

Corresponding Authors: D.P. McDonnell, Duke University School of Medicine, LSRC BLDG RM C238, Box 3813 DUMC, Durham, NC 27710. Phone 919-684-6035; Fax 919-681-7139; E-mail: Donald.mcdonnell@duke.edu; or S.J. Freedland, Cedars-Sinai Medical Center, 8635 West 3rd Street, Suite 1070W, Los Angeles, CA 90048. Phone: 310-423-3497; Fax: 310-423-4711; E-mail: stephen.freedland@cshs.org

doi: 10.1158/0008-5472.CAN-16-2738

cholesterol by inducing the expression of genes such as HMGCR and the low-density lipoprotein receptor (LDLR). Targeting these pathways has been shown to be an effective strategy to inhibit growth in relevant cellular and animal models of prostate cancer (28, 29).

Considering what is known about the pathobiology of cholesterol in prostate cancer, it is clear that these cancer cells have evolved mechanisms to bypass the tight homeostatic regulation of intracellular cholesterol, and this represents a potential vulnerability for intervention. With this idea in mind, we sought to identify genes involved in cholesterol homeostasis whose expression was dysregulated in prostate cancer. We reasoned that such an approach would also yield novel targets, which could be pharmaceutically exploited to have useful clinical activity. To achieve this goal, a list of genes with known involvement in cholesterol homeostasis was assembled with each gene being ranked according to the strength of the correlation between its expression level and prostate cancer clinical outcomes using publically available data. Using this approach, it was determined that the expression of CYP27A1, a gene that encodes sterol 27-hydroxylase, a cytochrome P450 oxidase that converts cholesterol into 27-hydroxycholesterol (27HC), was dramatically downregulated in prostate cancer when compared with benign prostate tissue (30). Although most cholesterol is catabolized by CYP7A1 in the liver, CYP27A1 is the rate-limiting step in the alternate or "acidic pathway" of bile acid synthesis. Further, it has been shown that 27HC, secondary to its interaction with INSIG-2 in the endoplasmic reticulum, inhibits the processing events required for the activation of SREBP2 (31). In this manner, 27HC serves as a component of a negative feedback loop that regulates cholesterol biosynthesis. Further, 27HC, functioning as an LXR agonist, can also enhance cholesterol efflux by upregulating the transcription of cholesterol transporters to further limit cellular cholesterol accumulation. However, the significance of this regulatory loop in prostate cancer pathogenesis has not been established. In this study, a combination of bioinformatics, genetics, and pharmacology has been used to determine the importance of CYP27A1 and 27HC in cholesterol homeostasis in prostate cancer. Further, it is shown that dysregulation of CYP27A1 expression and its metabolite (27HC) can affect the pathobiology of prostate cancer. Together, these studies also highlight the potential clinical utility of restoring cholesterol homeostasis in prostate cancer as a means to treat or prevent this disease.

Materials and Methods

Bioinformatic analysis
Association of CYP27A1 expression with prostate cancer clinical features. Using logistic regression in R, expressions of genes involved in cholesterol regulation (derived from gene ontology analysis) extracted from The Cancer Genome Atlas (TCGA) were assessed for their ability to predict Gleason score (6, 7, 8, >9), pathologic T-Stage (t2a, t2b, t2c, t3a, t3b, t4), and pathologic N-Stage(n0, n1) with each clinical feature modeled as an ordered factor. ORs, confidence intervals (CI), and two-tailed P values were calculated using R.

CYP27A1 mRNA levels and Gleason score. These results are based upon data generated by the TCGA Research Network: http://cancergenome.nih.gov/. Normalized gene expression data and clinical information for TCGA-Prostate Adenocarcinoma (PRAD)

were downloaded from The Broad Institute TCGA GDAC Firehose at http://gdac.broadinstitute.org. At the time of data access, 269 primary tumor samples were annotated for both gene expression and clinical data. Gleason score data were then categorized into three groups (Gleason score <7, =7, or >7). P values were determined using a one-way ANOVA.

PSA-free survival analysis for CYP27A1 mRNA. The raw data for GSE21032 were downloaded from GEO, normalized with Robust Multi-array Average approach, and summarized at the transcript level using the oligo package in R. Biochemical recurrence in this dataset was defined as PSA ≥ 0.2 ng/mL on two occasions. The Kaplan–Meier plot of PSA-free survival was generated in R with patients categorized into low and high *CYP27A1*-expressing groups according to the median expression of *CYP27A1*. Reported P values were calculated using the log-rank method.

CYP27A1 mRNA levels and promoter methylation. Data from TCGA-PRAD, representing 246 patient samples, were used to correlate transcription start site (TSS) methylation levels with mRNA expression levels of *CYP27A1*. The intensity of the proximal TSS probe of *CYP27A1* from the Infinium HumanMethylation450 BeadChip was plotted against the Log_2 mRNA *CYP27A1* expression levels from RNA-Seq. Data points were fitted with a loess smoothing curve.

CYP27A1 IHC analysis
The patient cohort and details of TMA construction were previously described (32). TMA sections were stained with anti-CYP27A1 rabbit monoclonal antibody (ab126785 from Abcam), and detailed protocol can be found in Supplementary Materials and Methods. Staining intensity in tumor cells was scored prospectively as 0 (absent), 0.5 (borderline), 1 (weak), 2 (moderate), or 3 (strong) by a board-certified pathologist (J. Geradts) blinded to clinical information. For statistical analysis, the tumors were categorized as negative (0 and 0.5) or positive (1, 2, and 3). A χ^2 test was used to test association between expression of CYP27A1 (treated as a binary variable) and PRAD versus benign tissue.

Cell culture and *in vitro* assays
Cell lines and culture conditions. LNCaP, 22RV1, DU145, and VCaP cells were obtained from the ATCC and were authenticated by the ATCC using short tandem repeat (STR) profiling. LAPC4 cells were a generous gift from Dr. William Aronson (UCLA, CA) and authenticated by the ATCC using STR profiling. All cell lines were passaged in the laboratory for no more than 20 passages (or 4 months). LNCaP and 22RV1 cells were cultured in RPMI-1640; DU145 in MEM; VCaP, 293FT, and 293Ts in DMEM; and LAPC-4 in Iscove's DMEM supplemented with 0.1 nmol/L R1881. All media were also supplemented with 10% FBS, 1 mmol/L sodium pyruvate, and 0.1 mmol/L NEAA. Q6

Gene silencing. LNCaP cells were seeded at 3×10^5 cells per well on a 6-well plate and transfected with siRNA as indicated using Dharmafect I (Dharmacon) for 48 to 72 hours, unless otherwise specified.

Generation of stable cell lines. pLenti CMV TRE3G puro Gal4-DBD and pLenti CMV TRE3G puro CYP27A1 were cotransfected (Fugene, Promega) with the vsvg, gag-pol, and rev packaging

194 vectors into 293FT cells. The viral supernatants were filtered and
195 supplemented with 8 µg/mL polybrene before infecting LNCaP or
196 22RV1 cells that constitutively express the pLenti CMV-rtTA3G
197 plasmid under blasticidin antibiotic selection. Cells were then
198 selected with 1 µg/mL puromycin yielding Gal4- and CYP27A1-
199 overexpressing cell lines.

200 *LDLR overexpression.* pQCXIP or pQCXIP LDLR were cotrans-
201 fected with the vsvg packaging vector into 293Ts cells. The viral
202 supernatants were filtered and supplemented with 8 µg/mL poly-
203 brene before infecting LNCaP cells. Forty-eight hours following
204 infection, LNCaP cells were harvested and plated for proliferation
205 assays.
206   Western blotting, RNA preparation, qRT-PCR analyses, and
207 proliferation assays were described previously (33–35).

208 *Anchorage-independent growth.* Anchorage-independent growth
209 was assessed by monitoring colony formation after 4 to 5 weeks in
210 soft agar (0.6% base; 0.3% top layer) using 5,000 cells per well in
211 6-well plates. Briefly, 0.6% agar (2 mL) in growth medium was
212 added to a 6-well plate and allowed to solidify. Then, cells were
213 suspended in 2 mL of 0.3% agar with or without 27HC (1 µmol/L)
214 and were added on top of the agar base and allowed to solidify.
215 Media containing DMSO or 27HC (1 µmol/L) were added to each
216 well, and treatment was replaced every 3 days. Colonies were
217 stained with crystal violet and counted using a phase contrast
218 microscope.

219 *Apoptosis assay.* LNCaP and 22RV1 cells (3×10^5 cells/well) were
220 seeded in 6-well plates and treated accordingly. Cells were then
221 harvested and double stained with Alexa Flour 488 Annexin V and
222 Sytox according to the manufacturers' instructions. Annexin V–
223 positive cells were considered apoptotic, and the percentage of
224 total cell number was calculated. A minimum of 10,000 events
225 were collected per sample using a BD Accuri C6 flow cytometer,
226 and data were analyzed using the CFlow plus program software
227 (BD Biosciences).

228 *Caspase 3/7 activity assay.* The assay was performed as described in
229 Fritz and colleagues (36) with modifications (see Supplementary
230 Materials and Methods).

231 *27HC and cholesterol measurements.* 27HC and cholesterol mea-
232 surements were performed by the Duke Proteomics and Metabo-
233 lomics Shared Resources. For details, see Supplementary Materials
234 and Methods.

235 **Murine tumor xenograft model**
236   All xenograft procedures were approved by the Duke University
237 Institute for Animal Care and Use Committee. Castrated Nod
238 Scid/Gamma (NSG) mice (∼6 weeks of age, $n = 20$ per group)
239 obtained from the Cancer Center Isolation Facility (Duke Cancer
240 Institute, Durham, NC) were subcutaneously injected with $1 \times$
241 10^6 22RV1-Gal4 or 22RV1-CYP27A1 cells into the right flank in
242 200 µL of a 50% mixture containing RPMI 1640 medium and
243 Matrigel matrix basement membrane (BD Corporation). Doxy-
244 cycline was added to the drinking water 2 days prior to xenograft
245 injections. Tumors were measured by caliper 2 to 3 times/week for
246 30 days after engraftment. At sacrifice, the tumors were harvested,
247 weighed, and flash-frozen for subsequent analysis of RNA, pro-
248 tein, and cholesterol.

Results 250

Cholesterol availability influences the growth of prostate cancer cells *in vitro* 251 252

As a first step in these studies, we assessed the impact of 253
manipulating cholesterol levels on prostate cancer growth. 254
More specifically, the consequence of altering media LDL levels 255
(the lipoprotein with the highest cholesterol content) on the 256
growth of prostate cancer cells was evaluated. To this end, VCaP 257
cells were cultured in media with lipoprotein-deficient serum 258
(LPDS), and their proliferation was assessed and compared 259
with cells grown in full serum containing media. After 8 days, 260
cell number, as measured by relative DNA content, increased 261
1.3-fold in LPDS media versus a 3.4-fold increase in full serum 262
media (Supplementary Fig. S1A). Adding LDL to LPDS media 263
restored VCaP cell number to full serum media levels. Similar 264
trends were observed in DU145 and 22RV1 prostate cancer 265
cells, where LDL addition significantly enhanced growth when 266
compared with cells grown in LPDS media (Supplementary Fig. 267
S1B and S1C). These results established a relationship between 268
cholesterol availability and prostate cancer cell growth rate and 269
confirmed the importance of exogenous cholesterol for cancer 270
cell growth. 271

The expression of *CYP27A1*, a gene involved in cholesterol homeostasis, correlates strongly with prostate cancer clinical outcome 272 273 274

Given our specific interest in developing therapeutics that 275
target pathways involved in regulating cholesterol homeostasis, 276
we used a bioinformatic approach to identify cholesterol-relat- 277
ed genes whose expression correlated with aggressive prostate 278
cancer in annotated clinical datasets. Specifically, a list of 176 279
genes involved in cholesterol biology was derived using the 280
following GO ontologies: "GO:0006695" = cholesterol bio- 281
synthetic process, "GO:0042632" = cholesterol homeostasis, 282
"GO:0045540" = regulation of cholesterol biosynthetic pro- 283
cess, and "GO:0008203" = cholesterol metabolic process. 284
Using data extracted from TCGA, the expression level of each 285
of these genes relative to clinical features known to predict 286
outcome such as T-stage, Gleason score at diagnosis, and the 287
presence of lymph node metastasis was assessed. These genes 288
were modeled for their association to these clinicopathologic 289
features using logistic regression and evaluated using both the 290
97.5% CI, OR, and statistical significance. To account for 291
multiple testing, only genes with a P value less than 0.01 were 292
considered significant. Though this does not fully account for 293
multiple testing, we also did not want to miss important 294
observations. Importantly, only one gene, *CYP27A1*, was sig- 295
nificant for all three features with all three P values ≤ 0.001, and 296
ten genes (AKR1D1, APP, FDXR, LIPE, STAR, APOF, LBR, 297
MBTPS1, OSBPL1A, and SQLE) were significant for any two 298
features. Applying this strategy, using P values as a primary 299
selection criterion, low *CYP27A1* expression was determined to 300
be the most significant predictor ($P = 4.102E{-}08$) of high 301
Gleason score, the second most significant predictor of lymph 302
node involvement ($P = 8.220E{-}04$), and the sixth strongest 303
significant predictor ($P = 1.460E{-}03$) of high T-stage (Table 1). 304
To further dissect the relationship between low *CYP27A1* 305
expression and high Gleason score, patients were divided into 306
three groups; Gleason score <7, =7, or >7 and the expression of 307
CYP27A1 across the categories as reported in TCGA was 308

Q7 **Table 1.** *CYP27A1* expression is a strong predictor of adverse clinical features of prostate cancer

Gene	OR	CI	P value
Gleason score			
CYP27A1	0.26483	0.16–0.43	4.10E−08
APOF	0.25448	0.15–0.44	5.87E−07
SQLE	1.78670	1.39–2.29	4.79E−06
MBTPS1	0.74615	0.66–0.85	6.30E−06
CYP11A1	0.38565	0.25–0.61	3.82E−05
APP	0.59233	0.46–0.77	6.57E−05
AKR1D1	1.90077	1.32–2.73	0.00050
LIPE	0.59083	0.44–0.80	0.00065
SCARF1	1.46060	1.17–1.83	0.00095
STAR	0.64615	0.50–0.84	0.00097
Lymph node involvement			
FDXR	0.72412	0.61–0.85	0.00011
CYP27A1	0.59097	0.43–0.80	0.00082
LIPE	0.73486	0.61–0.89	0.00148
AKR1D1	1.44964	1.15–1.83	0.00195
APP	0.79939	0.68–0.94	0.00704
FDX1	1.11412	1.03–1.21	0.00910
LCAT	0.75251	0.61–0.93	0.00921
STAR	0.79685	0.67–0.95	0.00932
T-stage			
OSBPL1A	1.59274	1.23–2.05	0.00034
APOF	0.23175	0.10–0.54	0.00070
CLN8	0.61430	0.46–0.82	0.00091
MBTPS1	0.71497	0.59–0.87	0.00103
TNFSF4	1.84815	1.27–2.69	0.00129
CYP27A1	0.29065	0.14–0.62	0.00146
SQLE	1.85687	1.25–2.75	0.00204
INSIG2	1.43199	1.13–1.82	0.00332
PCSK9	2.47241	1.33–4.59	0.00418
LBR	1.56478	1.15–2.13	0.00426

NOTE: Expression of genes involved in cholesterol regulation (derived from gene ontology analysis) was assessed for its ability to predict Gleason score at the time of diagnosis, lymph node involvement, and T-stage. All the data were extracted from TCGA, and calculations were done with R-software. Only the ten most highly ranked genes are shown for each clinical feature out of a total 176 genes shortlisted through GO analysis.

assessed (Fig. 1A). Notably, *CYP27A1* mRNA expression levels were significantly lower in patients with Gleason score >7 versus patients with Gleason = 7 ($P < 0.0001$) or Gleason < 7 ($P < 0.0001$).

Using data extracted from seven different GEO datasets, we looked for differences in *CYP27A1* expression between the different stages of clinical and pathologic disease progression (benign, primary, metastatic, hormone sensitive, and hormone refractory); *CYP27A1* transcript levels were significantly lower in tumor samples versus benign prostate tissue across all five datasets that included benign and prostate cancer tissue (Fig. 1B; Supplementary Table S1; and Supplementary Fig. S1D). Moreover, in three of the four datasets that included data on metastasis, *CYP27A1* expression levels were significantly decreased in metastatic tumors versus primary tumors (Supplementary Table S2 and Supplementary Fig. S1D). The effect of transitioning to castrate-resistant prostate cancer (CRPC; aka hormone-resistant prostate cancer or HRPC) on *CYP27A1* expression was not as clear as one dataset showed significantly lower expression in HRPC (Tamura-GSE6811), whereas in a second dataset (Tomlins-GSE6099), no significant difference in expression was noted (Supplementary Table S3 and Supplementary Fig. S1D). Querying the TCGA-PRAD dataset revealed a strong negative correlation between the *CYP27A1* mRNA

levels and DNA methylation at the TSS of this gene (Fig. 1C). This analysis suggests that an epigenetic event may be involved in the silencing of CYP27A1 in prostate cancer.

To confirm that CYP27A1 expression was also reduced at the protein level, we assessed CYP27A1 protein using immunohistochemistry in tissue microarrays (TMA) that contained 1 mm cores from prostate cancer and benign prostate tissue. In these TMAs, the majority (89%; 106/119) of the benign cores expressed CYP27A1, whereas only 28% (28/101) of the cancer cores expressed CYP27A1 (χ^2, $P < 0.001$). A representative photomicrograph demonstrating the absence of CYP27A1 staining in tumor cells (black arrows) and positive staining in benign cells admixed within the cancerous cells (red arrows) is shown in Fig. 1D.

To test whether *CYP27A1* expression can predict clinical outcome, we queried the Taylor-GSE21032 dataset and found that patients whose tumors exhibited higher *CYP27A1* expression also had a significantly reduced risk of PSA recurrence following radical prostatectomy (HR = 0.325, $P = 0.00211$; Fig. 1E). Taken together, these data establish a negative correlation between CYP27A1 expression and prostate cancer progression.
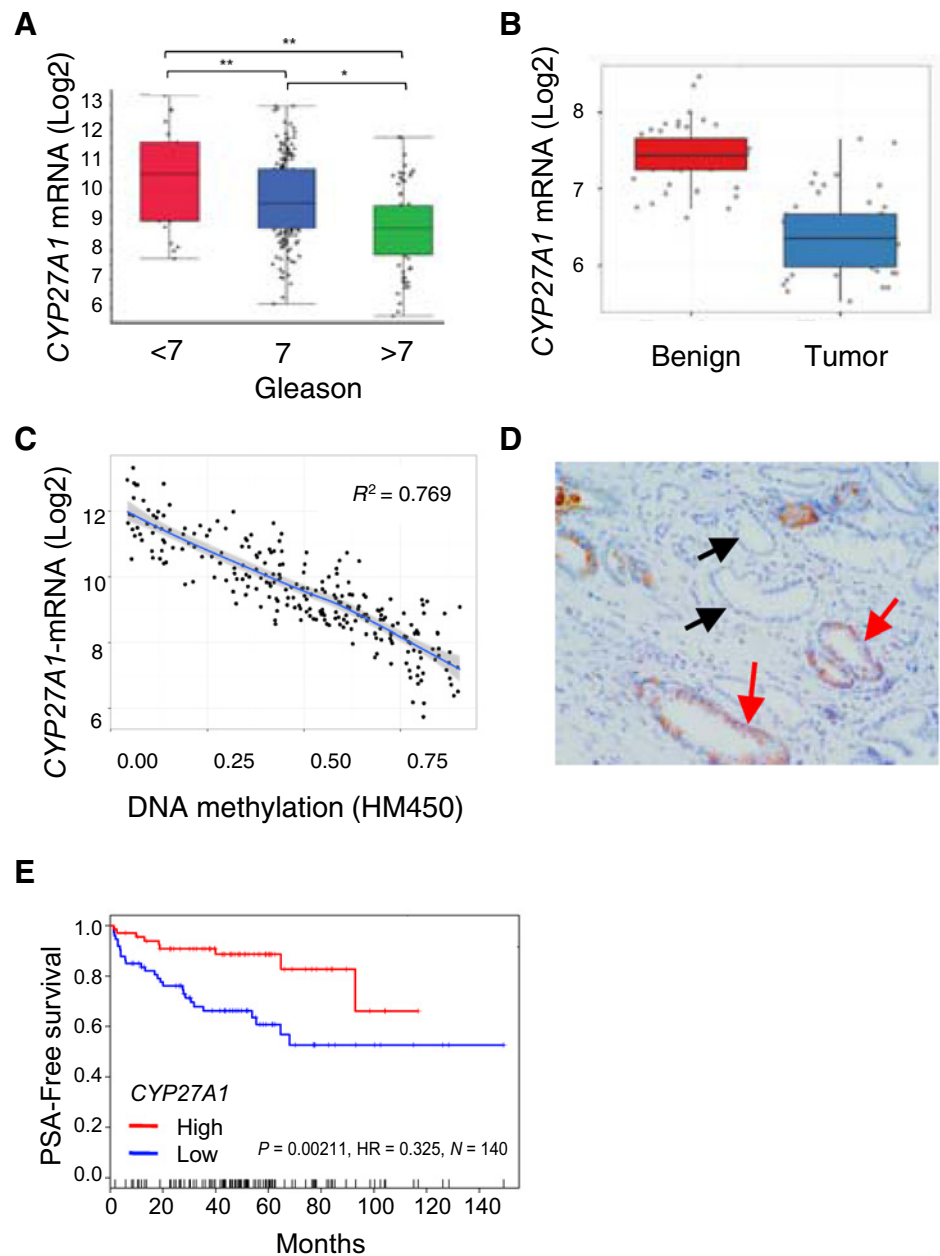
Restoration of CYP27A1 expression slows the growth of prostate cancer cells *in vitro* and attenuates the growth of 22RV1 cell–derived xenografts

Next, we wanted to determine whether altering CYP27A1 activity/levels affects prostate cancer cell growth. CYP27A1 expression was first assessed in six prostate cancer cell lines (DU145, PC3, LNCaP, 22RV1, LAPC4, and VCaP) by immunoblot analysis. As shown in Supplementary Fig. S2A, only the androgen receptor (AR)–negative DU145 and PC3 cells express detectable levels of CYP27A1 protein, although it is not known if this enzyme is active in these cells. As most prostate tumors express AR, even in late-stage CRPC (37), we elected to use the AR-expressing LNCaP and 22RV1 cells for further studies of CYP27A1 biology. LNCaP and 22RV1 cells were engineered to stably overexpress CYP27A1 or GAL4-DBD (control) both under the control of a doxycycline-inducible promoter. Doxycycline treatment resulted in a dose-dependent increase in CYP27A1 mRNA and protein expression in LNCaP and 22RV1 cells with enforced CYP27A1 expression but not in control cells (Supplementary Fig. S2B and S2C). Using the stably transfected cells described above, we assessed the effect of enforced CYP27A1 overexpression on prostate cancer cell growth *in vitro*. It was observed that the growth of cells expressing CYP27A1 was significantly impeded in both LNCaP and 22RV1 cells (Fig. 2A). Furthermore, these CYP27A1-expressing cells demonstrated significantly reduced ability to grow in an anchorage-independent manner (Fig. 2B).

22RV1 cells express a truncated, constitutively active, AR variant that confers resistance to all of the currently available androgen synthesis inhibitors and to antiandrogens and are a model of CRPC (38). Thus, considering the growth-inhibitory effects of CYP27A1 overexpression on 22RV1 cells *in vitro*, the effect of CYP27A1 overexpression on the growth of 22RV1 cell–derived tumors was evaluated *in vivo*. To this end, 22RV1 control cells (expressing GAL4) or those that overexpress CYP27A1 were propagated as xenografts in castrated, immunodeficient mice, and tumor growth was assessed by caliper measurements. Two days prior to injection of tumor cells, mice were given doxycycline in their drinking water (Supplementary Fig. S2D). Starting at day

Figure 1.
CYP27A1 is lost in prostate cancer and predictive of progression. **A,** TCGA was queried for mRNA levels of *CYP27A1* in tumor samples, and Gleason score at the time of diagnosis. Patients whose tumors have a Gleason score >7 have significantly lower levels of expression of *CYP27A1* than patients whose tumors have a Gleason score = 7 or a Gleason score <7. *, $P < 0.05$; **, $P < 0.0001$. **B,** Data from Brase (GSE29079) was queried for mRNA levels of *CYP27A1*. *CYP27A1* transcript levels are significantly lower in tumor versus benign samples ($P = 2.84e–19$). **C,** Data from TCGA-PRAD, representing 246 patient samples, were used to correlate TSS methylation levels with mRNA expression levels of *CYP27A1*. **D,** A representative photomicrograph of a cancerous prostate core immunostained for CYP27A1 displays no staining for CYP27A1 in the malignant epithelium (black arrows). Benign glandular epithelium admixed in the core displays moderate staining for CYP27A1 (red arrows). **E,** The association of tumor levels of CYP27A1 on patient survival was queried using the Taylor (GSE21032) clinical dataset. In this analysis, biochemical recurrence following radical prostatectomy was used as the primary end point. Kaplan–Meier curves generated for cancer patients with *CYP27A1* expression above or below the median indicate that patients whose tumors express higher levels of *CYP27A1* (above the median) have significantly delayed recurrence ($P = 0.00211$).
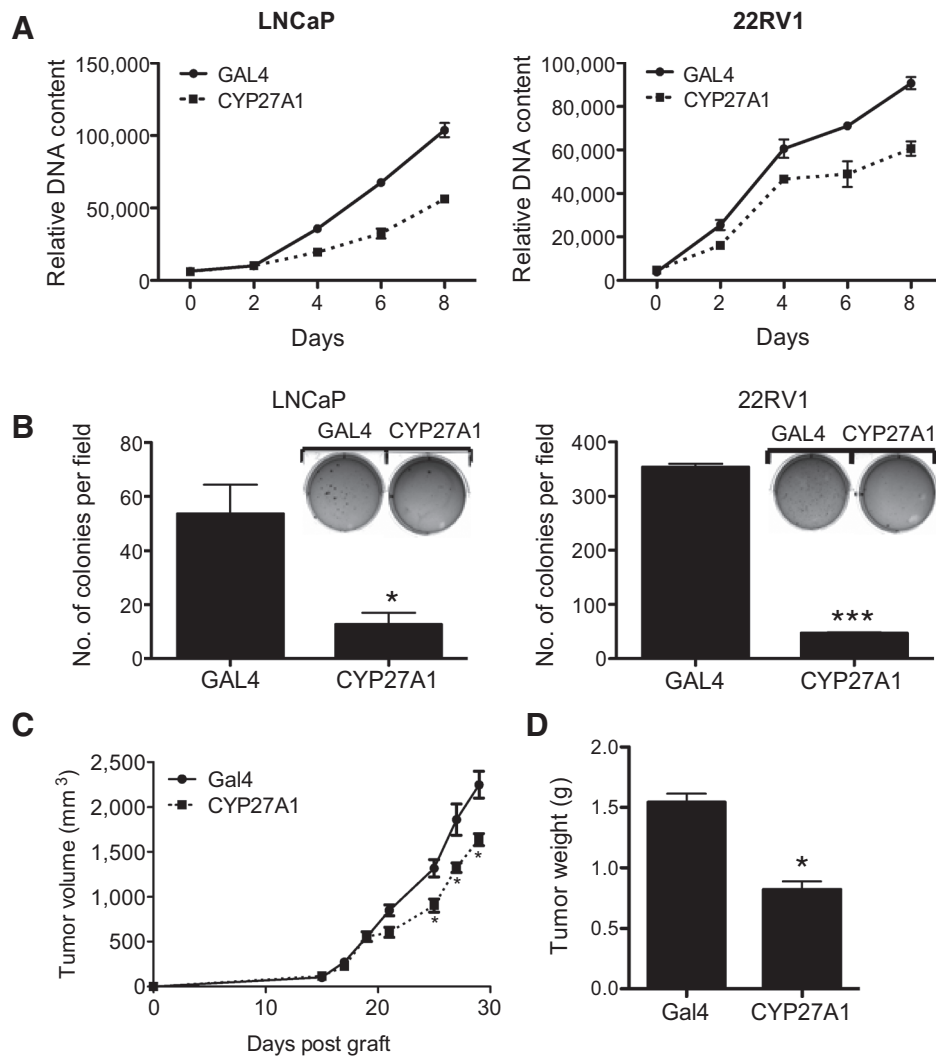
Q8

25 and continuing through the remainder of the study, tumors expressing CYP27A1 were significantly smaller than those expressing GAL4 (Fig. 2C). At sacrifice, the weight of tumors derived from the CYP27A1-expressing cells was half that of tumors expressing GAL4 (Fig. 2D). Tumoral expression of CYP27A1 was confirmed by immunoblot analysis (Supplementary Fig. S2E). It was concluded from these studies that restoring CYP27A1 levels negatively affects prostate cancer growth *in vitro* and *in vivo*.

CYP27A1 inhibits the growth of prostate cancer cells via production of 27HC

The *CYP27A1* gene encodes a cytochrome P450 oxidase, sterol 27-hydroxylase, the primary activity of which is to convert cholesterol into 27HC (30). In addition, however, it has been shown that recombinant CYP27A1 has weak vitamin D 25-hydroxylase activity and, when assessed *in vitro*, can convert vitamin D3 (calciferol) into 25-hydroxyvitamin D_3 ($25(OH)D_3$) (39). This is of potential significance as $25(OH)D_3$ can be converted to $1,25$-dihydroxyvitamin D_3 ($1,25(OH)_2D_3$) by CYP27B1, a seco-steroid that has been shown to inhibit the growth of many different cancer cells. Thus, to assess the extent to which the inhibitory effects of CYP27A1 overexpression in PCa cells can be attributed to the production of $1,25(OH)_2D_3$, we analyzed the expression of several genes which read on vitamin D receptor (VDR) activity in cells upon induction of CYP27A1 expression (Supplementary Fig. S3). As expected, treatment with $1,25(OH)_2D3$ robustly induced the expression of several VDR target genes, such as TMPRSS2 and CYP24A1, at concentrations as low as 1 nmol/L. However, overexpression of CYP27A1 had no effect on the expression of these VDR targets ruling out the possibility that
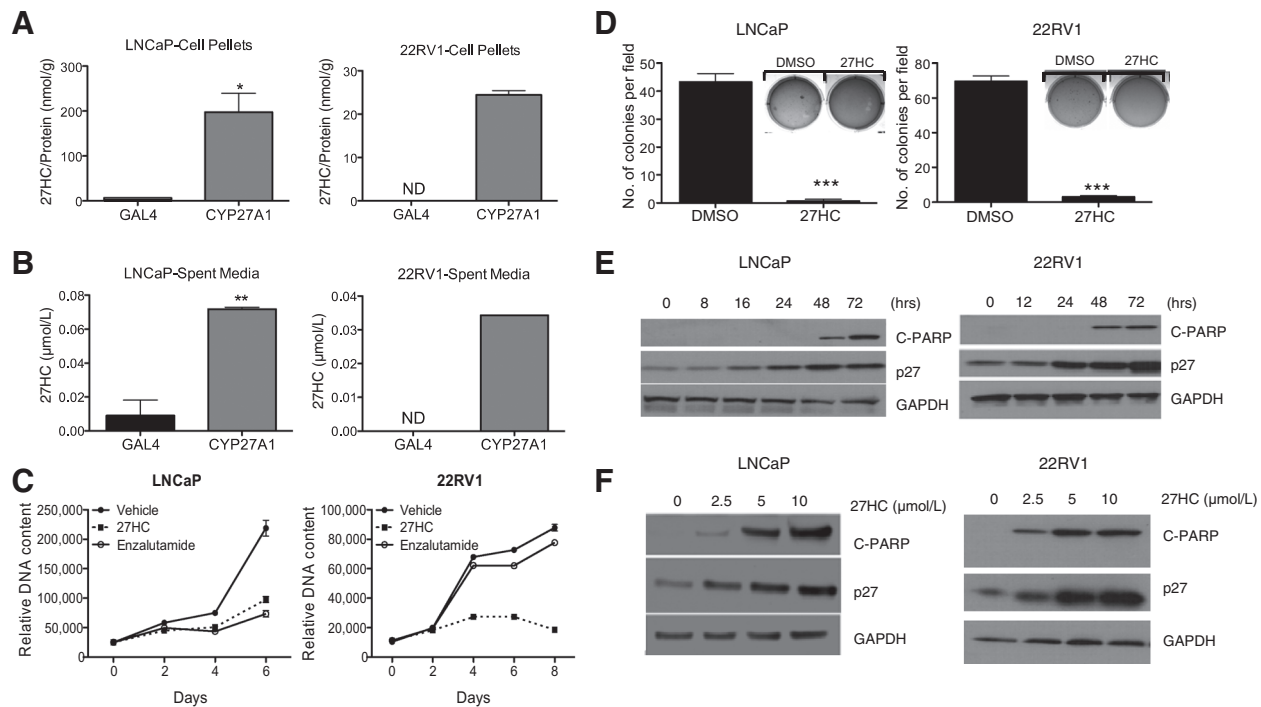
Q9

Figure 2.
27HC inhibits the growth of prostate cancer cells *in vitro* and in xenografts. **A,** LNCaP or 22RV1 cells stably expressing CYP27A1 or its GAL4 control were plated in full serum media. Twenty-four hours later, cells were treated with 25 ng/mL of doxycycline. Cells were then harvested at the indicated days and DNA content measured using Hoechst 33258. The data shown are a representative of three independent experiments. **B,** LNCaP or 22RV1 cells stably overexpressing CYP27A1 or GAL4 control were treated with doxycycline. Two days later, cells were seeded in soft agar in 6-well plates and incubated for 3 weeks. Colonies were stained with crystal violet. Graph represents the number of colonies growing in soft agar per microscopic field. Three different microscopic fields were counted per well. Experiments were done 3 times. Error bars represent the SEM; *, $P < 0.05$; **, $P < 0.001$ (unpaired t test). A representative well showing colonies growing in soft agar is also shown in the graph. **C,** Growth curve of GAL4- and CYP27A1-overexpressing tumors. 22RV1 cells (1×10^6) that stably expressed CYP27A1 or GAL4 (control) were implanted into the flanks of castrated NSG mice ($n = 20$ per group) and followed for tumor growth by calipers. Two days prior to tumor injection, mice were given doxycycline in the drinking water to induce CYP27A1 and GAL4 expression. Starting at day 25 after engraftment and continuing through the remainder of the study, tumors overexpressing CYP27A1 were significantly smaller than tumors overexpressing GAL4 (*, $P < 0.05$, Bonferroni T test following two-way ANOVA). **D,** Graph representing mean of the weights of GAL4- and CYP27A1-overexpressing tumors harvested at sacrifice (*, $P < 0.05$, t test).

functionally significant levels of $1,25(OH)_2D_3$ were being produced upon reexpression of this enzyme. Notably, however, the expression of CYP27A1 resulted in increased production of intracellular 27HC in both LNCaP and 22RV1 cells when compared with control cells (Fig. 3A). A commensurate increase in 27HC in the spent media from CYP27A1-expressing cells was also observed (Fig. 3B). Because CYP27A1 overexpression inhibited prostate cancer cell growth, we next sought to determine if 27HC treatment results in a similar outcome. To this end, we compared the effects of 27HC on LNCaP and 22RV1 cell growth. Enzalutamide, an antiandrogen used to treat advanced prostate cancer, was used as a control. 27HC inhibited the growth of both LNCaP and 22RV1 cells, whereas enzalutamide inhibited the growth of only LNCaP but not 22RV1 cells as expected, as these later cells express an AR splice variant(s) that confers resistance to antiandrogens (Fig. 3C; refs. 40, 41). An even more dramatic inhibitory effect of 27HC on anchorage-independent growth of prostate cancer was observed (Fig. 3D). Treatment of LNCaP and 22RV1 cells with 27HC was associated with a dramatic increase in cleaved PARP (marker of apoptosis), and p27 (marker of cell-cycle arrest) in a time- and

Figure 3.
27HC, produced by CYP27A1 in prostate cancer, slows the growth of prostate cancer cells *in vitro* and induces molecular markers of apoptosis and cell-cycle arrest. **A,** LNCaP and 22RV1 cells overexpressing CYP27A1 or its GAL4 control were plated and treated with doxycycline (25 ng/mL) for 7 days. 27HC levels were measured using a targeted LC-MS/MS method (see Materials and Methods) and normalized to total protein. Experiment was repeated 3 times, and error bars represent SEM (*, P < 0.05, unpaired *t* test). ND, not detectable (detection limit: 0.03 μmol/L) **B,** 27HC levels in spent media were measured as in **A** (*, P < 0.05, unpaired *t* test). **C,** Cells were seeded in 96-well plates for 24 hours and then treated with either 5 μmol/L of 27HC, 5 μmol/L of enzalutamide, or vehicle control (DMSO). Cells were harvested at the indicated days, and final DNA content was determined by staining with the DNA dye Hoechst 33258. The data shown are representative of three independent experiments. **D,** Cells were seeded in soft-agar plates and incubated for 3 weeks in the presence of vehicle (DMSO) or 1 μmol/L 27HC. Colonies were stained with crystal violet. Graph represents the number of colonies per microscopic field. Three different microscopic fields were counted per well. Experiments were done 3 times. Error bars represent the SEM and ***, P < 0.0001 (unpaired *t* test). A representative well showing colonies growing in soft agar is also shown in the graph. **E,** Cells were plated in 6 cm dishes and treated with 10 μmol/L 27HC the next day. Cell lysates were harvested at the indicated time points, and immunoblot analysis was performed to analyze expression levels of cleaved PARP (C-PARP) and p27. GAPDH was used as a loading control. **F,** Cells were treated with 27HC (2.5, 5, or 10 μmol/L) or vehicle control (DMSO) for 72 hours, and immunoblot analysis was performed as in **E**.
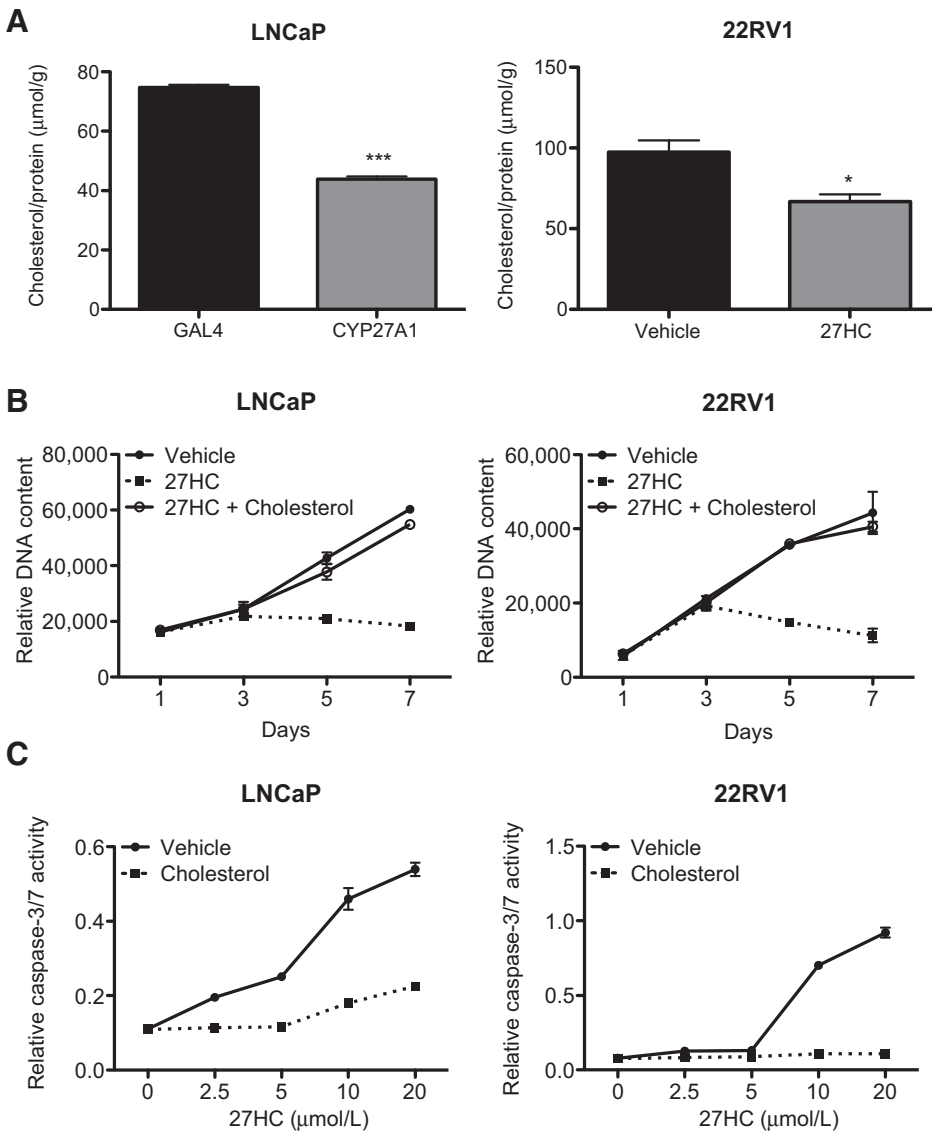
dose-dependent manner (Fig. 3E and F), and corresponding increases in apoptosis (Supplementary Fig. S5D). Analogous findings were observed when VCaP (AR amplified) and DU145 (AR null) cells were treated in a similar manner (Supplementary Fig. S4A and S4D). It was noted, however, that 27HC treatment resulted in the induction of cleaved PARP in VCaP cells but not in DU145 cells (Supplementary Fig. S4B and S4C and data not shown). Conversely, 27HC treatment resulted in the induction of p27 expression in DU145 but not in VCaP cells (Supplementary Fig. S4E and S4F and data not shown). The molecular basis for these differences is presently unclear, although all of the data are consistent with 27HC having a negative effect on prostate cancer viability irrespective of AR status.

27HC inhibits growth of prostate cancer cells via depletion of intracellular cholesterol

Some oxysterols, including 27HC, have been shown to participate in a negative feedback loop that is responsible for regulating cholesterol biosynthesis (31). To determine if the CYP27A1/27HC axis is involved in cholesterol homeostasis in prostate cancer cells, we first assessed the impact of 27HC administration on cholesterol levels in prostate cancer. As shown in Fig. 4A, treatment of prostate

cancer cells with 27HC resulted in a significant decline in cellular cholesterol in both LNCaP and 22RV1 cells by 35% (P = 0.00152) and 28% (P = 0.00388), respectively. Similar decreases in cellular cholesterol content were also observed in CYP27A1-overexpressing LNCaP cells but not in 22RV1 cells (Supplementary Fig. S5A). However, a significant decrease in total cholesterol was noted in CYP27A1-overexpressing 22RV1 tumors (Supplementary Fig. S5B). This latter discrepancy may relate to differences in the reliance on cholesterol synthesis versus uptake by these cells when propagated *in vitro* and *in vivo*.

A cholesterol complementation study was done to determine whether depletion of cholesterol is sufficient to explain the inhibitory effect of 27HC on prostate cancer growth. Indeed, the growth-inhibitory effects of 27HC on LNCaP and 22RV1 cells were reversed by adding exogenous cholesterol (Fig. 4B). Further, cholesterol supplementation reversed 27HC-dependent (a) induction of PARP cleavage (Supplementary Fig. S5C), (b) increases in the activity of effector caspases 3 and 7 (Fig. 4C), and (c) apoptosis (Supplementary Fig. S5D). Likewise, pretreating LNCaP or 22RV1 cells with LDL for 48 hours prior to the addition of 27HC significantly attenuated the antiproliferative effects of 27HC (Supplementary Fig. S5E). These data are consistent with

Figure 4.
27HC inhibits growth of prostate cancer cells via depletion of cellular cholesterol. **A,** LNCaP or 22RV1 cells were treated with 10 μmol/L of 27HC. Three days later, the cells were harvested, and cell lysates were extracted with RIPA buffer. Cellular levels of cholesterol were quantified using a targeted LC-MS/MS method (Materials and Methods). Experiment was repeated 3 times. Error bars represent the SEM and *, $P < 0.05$ was considered a significant variation (unpaired t test). **B,** LNCaP or 22RV1 cells were plated in 96-well plates. One day later, the cells were treated with 5 μmol/L 27HC in the presence or absence of 10 μmol/L cholesterol. Cells were harvested at the indicated days, and cell numbers were determined by staining with the DNA dye Hoechst 33258. The data shown are representative of three independent experiments. **C,** LNCaP or 22RV1 cells were plated in 96-well plates. One day later, the cells were treated with the indicated doses of 27HC in the presence or absence of 10 μmol/L cholesterol. Caspase 3/7 activity was measured 48 hours later using a luminescent based assay. Caspase activity was normalized to DNA content of the cells stained with Hoechst 33258 measured from a parallel experiment. The data shown are representative of three independent experiments.

the idea that 27HC-mediated effects on cell growth are a result of reduced cellular cholesterol content.

27HC-dependent inhibition of prostate cancer cell growth occurs via downregulation/inhibition of SREBP2 activity

In light of the observation that direct addition of 27HC, or overexpression of CYP27A1, reduced cellular cholesterol content and inhibited cell growth, it was of interest to define the mechanisms by which 27HC affected cholesterol homeostasis. As mentioned above, the levels of cholesterol in cells are regulated by uptake, efflux, and biosynthesis primarily through the coordinated activity of SREBPs and LXRs (24–26). Therefore, the ability of 27HC to affect the expression of canonical LXR and SREBP target genes was assessed. Treatment of LNCaP and 22RV1 cells with 27HC resulted in the upregulation of ABCG1 and a downregulation of LDLR mRNA expression (Fig. 5A and data not shown). The magnitude of the induction of ABCG1 expression by 27HC is similar to that achieved with the synthetic LXR agonist T0901317 (T1317),

and depletion of LXRα and β isoforms by siRNA diminished this induction (Fig. 5A). This suggests upregulation of ABCG1 by 27HC is mediated by LXRs. On the other hand, downregulation of LDLR by 27HC was independent of the LXRs as knockdown of LXRs did not rescue LDLR downregulation (Fig. 5A, right).

To determine the role of LXRs as a mediator of the growth-inhibitory effects of 27HC on prostate cancer cells, the ability of the synthetic LXR agonist T1317 to phenocopy the effects of 27HC on in vitro growth of LNCaP and 22RV1 cells was assessed. Like 27HC, T1317 significantly inhibited the growth of LNCaP cells. However, 22RV1 cells which are 27HC responsive were not inhibited by T1317 even at doses as high as 10 μmol/L (Fig. 5B). Thus, although 27HC can function as an LXR agonist in prostate cancer cells, its actions on overall cholesterol homeostasis and on cell proliferation are likely to occur, at least in part, in an LXR-independent manner. Therefore, we assessed if SREBP2, which is also known to be involved in cholesterol homeostasis, was a mediator of the 27HC anti–prostate cancer effects. As shown
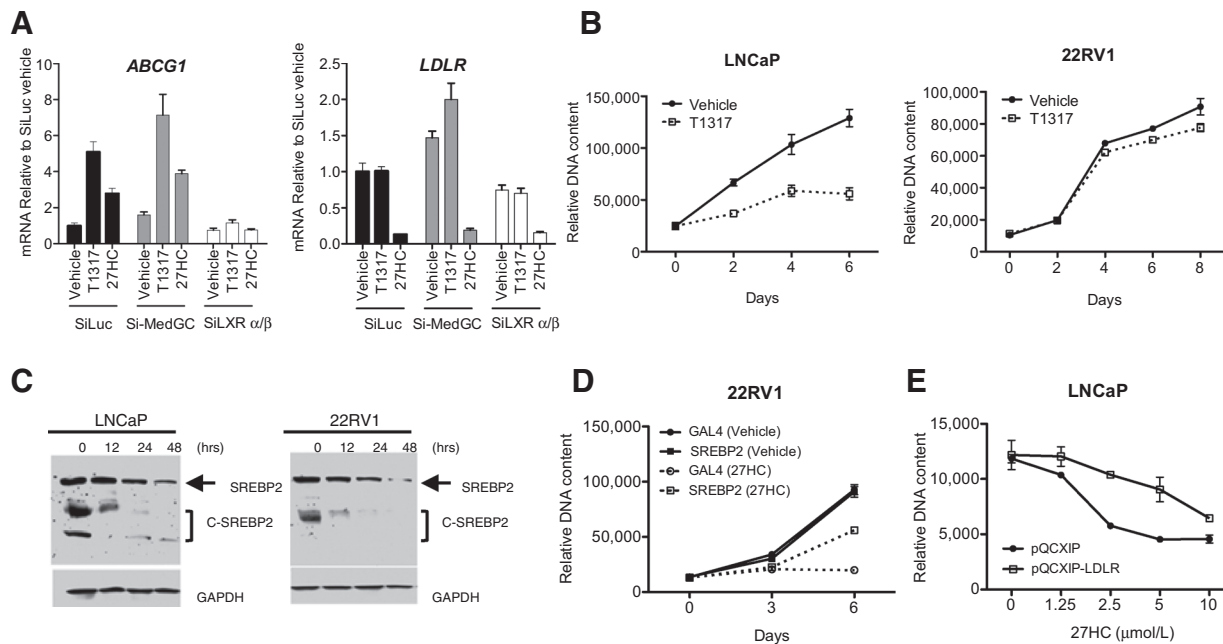
Figure 5.
27HC-dependent inhibition of prostate cancer cell growth occurs via downregulation/inhibition of SREBP2 activity. **A,** LNCaP cells were transiently transfected with siRNA targeting Si-Luc (negative control), or MED-GC (negative control), or LXRs (LXR-α and LXR-β). Two days later, the cells were treated with vehicle, or 27HC (10 μmol/L), or T1317 (10 μmol/L) for 18 hours. The expression of *ABCG1* and *LDLR* was assessed using qPCR. Data are presented as fold induction above vehicle-treated cells. The data shown are representative of three independent experiments. **B,** LNCaP or 22RV1 cells were plated in 96-well plates. The next day, cells were treated with T1317 (10 μmol/L) or vehicle control and harvested at the indicated time points. The DNA content of the cells was measured by Hoechst 33258. **C,** Cells were treated with 5 μmol/L of 27HC and harvested at the indicated time points. Immunoblot analysis was performed to analyze expression levels of SREBP2, using an antibody specific to its C-terminus, and GAPDH (loading control). The arrow indicates precursor (full-length) form of SREBP2. Several smaller cleaved/processed forms of SREBP2 were also detected in the cell lysate (bracketed, C-SREBP2). **D,** 22RV1 cells that stably express active fragment of SREBP2 (N-terminus) or GAL4 control were plated in 96-well plates and treated with doxycycline (25 ng/mL) for 24 hours. The cells were then treated with 27HC (2.5 μmol/L) or its vehicle control and harvested on the indicated days following treatment. Final DNA content of the cells was determined as in **B**. The data shown are representative of three independent experiments. **E,** LNCaP cells were transiently infected with a retrovirus that carries LDLR (PQCXIP-LDLR) or an empty vector as a negative control (PQCXIP-CTRL). Forty-eight hours later, cells were harvested and a proliferation assay was performed in the presence of the indicated doses of 27HC. Seven days later, cell numbers were determined by staining with the DNA dye Hoechst 33258. The data shown are representative of three independent experiments.

in Fig. 5C, treatment with 27HC led to a time-dependent decrease in the levels of the precursor form of SREBP2 in LNCaP and 22RV1 cells, consistent with the downregulation of SREBP2 mRNA expression by 27HC (data not shown). This is likely due to the fact that SREBP2 activity is required for its own transcription (42). We next tested whether the effects of 27HC on cell growth can be reversed by exogenously expressing the active nuclear form of SREBP2 (43, 44). For this purpose, 22RV1 cells engineered to stably overexpress the active form of SREBP2 or GAL4 (control) under the control of a doxycycline-inducible promoter were developed. Overexpression of SREBP2 significantly reduced the sensitivity of 22RV1 cells to 27HC (Fig. 5D). Because LDLR is a major downstream target of SREBP2, we evaluated whether LDLR overexpression alone could abrogate 27HC-mediated antiproliferative effects. Indeed, LNCaP cells that were transiently infected with an LDLR-expressing retrovirus were found to have an attenuated response to 27HC (Fig. 5E). Finally, we demonstrated that siRNA-mediated knockdown of LDLR expression phenocopied the effects of 27HC on prostate cancer growth (Supplementary Fig. S6A–S6C). It was concluded from these studies that 27HC-dependent downregulation of SREBP2 activity and LDLR expression in part explains the antiproliferative effects of 27HC on prostate cancer.

Discussion

The results of this study provide a potential mechanistic link between dysregulated cholesterol homeostasis and prostate cancer pathogenesis and highlight approaches that can be used to mitigate the impact of dyslipidemia on the biology of this disease. Notable was our observation that the expression of CYP27A1, a key component of the cellular cholesterol homeostatic machinery, was dramatically downregulated in advanced prostate cancer, an activity that may result from hypermethylation of the gene encoding this protein. Absent this enzyme, an important negative feedback mechanism that regulates cellular cholesterol homeostasis is lost leading to cholesterol accumulation, which endows a selective growth advantage upon prostate cancer cells (Supplementary Fig. S6D). Whereas the mechanisms by which increased cholesterol synthesis/uptake affects prostate cancer cell growth remain under investigation, it is clear from our studies that restoration of the activity of the CYP27A1/27HC signaling axis and/or modalities that decrease cellular cholesterol content are likely to have a positive impact on prostate cancer treatment/prevention.

In addition to the data presented here, other preclinical studies have shown that intratumoral cholesterol homeostasis and

negative feedback loops are deregulated in prostate cancer (45–47). For example, *LDLR* mRNA and SREBP2 expressions are downregulated in the presence of exogenous LDL or cholesterol in normal prostate cells but not in the prostate cancer cells (45). Although both normal and prostate cancer cells respond to low cholesterol media by upregulating cholesterol uptake and/or synthesis genes, prostate cancer cells have considerably lower expression of the cholesterol exporter ABCA1, thus potentially allowing them to accumulate more cholesterol (47). This supports the idea that prostate cancer cells have reprogrammed cholesterol homeostatic gene networks, which may enable them to become resistant to cholesterol-lowering drugs. Although this has not been tested directly in prostate cancers from patients on cholesterol-lowering drugs, a recent window of opportunity trial in breast cancer patients which showed that administration of atorvastatin, while lowering circulating cholesterol as expected, actually resulted in an upregulation of the expression of intratumoral HMGCR, the rate-limiting enzyme in cholesterol biosynthesis (48). This important clinical finding suggests that when faced with reduced availability of LDL-cholesterol, cancer cells can respond by increasing intracellular cholesterol production, a finding that questions whether lowering circulating cholesterol in and of itself would have a significant impact on the intracellular levels of cholesterol within cancer cells and thereby slow prostate cancer growth. It is intriguing to speculate that this fact explains why the epidemiologic data linking cholesterol and statin use and prostate cancer are mixed, with many studies suggesting no such link (49). Ultimately, future studies wherein both serum and intratumoral cholesterol are measured are required to test the true link between cholesterol and prostate cancer.

The findings of this study suggest that, as with other rapidly dividing cells, prostate cancer cells must have developed mechanisms to bypass the processes that regulate intracellular cholesterol content to enable them to accumulate cholesterol that has been shown to constitute an important checkpoint in cell division (50). We believe, given what is known about the role of oxysterols in the negative feedback control of cholesterol biosynthesis/uptake, that prostate cancer cells accomplish this activity by blocking the synthesis of 27HC as a consequence of CYP27A1 gene silencing. In support of this hypothesis, we have shown that ectopic expression of CYP27A1 in prostate cancer cells decreases cellular and intratumoral cholesterol accumulation and inhibits cell/tumor growth. Mechanistically, we have shown that 27HC mediates this effect in part through downregulation of SREBP2, which in turn suppresses *de novo* synthesis and uptake of cholesterol. In support of this model, we have shown that the growth-inhibitory activity of 27HC is considerably attenuated by ectopic expression of activated SREBP2 or by overexpression of LDLR from a heterologous promoter. Thus, it appears that downregulating CYP27A1 expression in prostate cancer cells interferes with an important negative feedback mechanism that enables these cells to accumulate the cholesterol needed for cell growth.

In addition to functioning as a partial agonist of LXRs and an inhibitor of SREBP2 activity, 27HC has also been shown to interact with estrogen receptors α and β (ERs; ref. 51). Both of these ERs have been reported to be expressed in prostate tissue, although their exact roles in prostate cancer development and progression remain unresolved (52). It has been shown that activation of ERβ is protective against prostate cancer (52, 53), a finding that may be significant given that 27HC has been shown to inhibit the transcriptional activity of both ER isoforms in the cardiovascular system but demonstrated partial agonist activity in the breast tissues. However, despite considerable effort, we were unable to detect significant expression of either ERs in any of the prostate cancer cell models used in our study (data not shown). This argues for the noted antiproliferative and proapoptotic effects of 27HC in prostate cancer are ER-independent. Notably, however, a recent article described an ER- and AR-dependent growth-promoting effect of 27HC in nontransformed RWPE-1 prostate epithelial cells (54). It remains to be determined whether this effect is due to the agonist activity of 27HC on ER in these cells, similar to what has been observed in breast cancer cells (34), or that 27HC has opposite effects in transformed versus nontransformed prostate epithelial cells.

In summary, like most rapidly dividing cells, prostate cancer cells need to bypass the tight homeostatic mechanisms that regulate the levels of intracellular cholesterol. The data presented in this study indicate that this can be accomplished in prostate cancer cells by downregulating the expression of CYP27A1, thus inhibiting the production of 27HC, a molecule involved in feedback control of cholesterol synthesis and uptake. It remains to be determined how this regulatory activity can be restored and/or how the effects of the increased cholesterol uptake that result from the loss of CYP27A1 expression can be mitigated. It is unlikely that statin use alone would have a significant effect, as it has been shown in other cancers that such an approach may lead to an upregulation of cholesterol biosynthesis in tumors (48). It would appear that the therapeutic options to target this pathway in cancer are limited to (1) the induction of the expression of genes involved in cholesterol efflux (such as LXR agonists), (2) approaches that reverse the inhibition of CYP27A1 expression/activity and (3) SREBP2 inhibitors or other compounds which interfere with cholesterol biosynthesis. It has been shown that LXR agonists can inhibit the growth of prostate cancer in animal models (55), the growth, and metastasis of melanoma (56), and we have also shown that they can decrease the growth of mammary tumors (34). Inhibitors of SREBP1/2 and oxidosqualene cyclase have also shown promise in preclinical models of prostate cancer (57, 58). Exploration of the viability of these approaches, especially in combination, as a means to mitigate cholesterol-enhanced cancer risk, is a focus of our continued research.

Disclosure of Potential Conflicts of Interest

No potential conflicts of interest were disclosed.

Authors' Contributions

Conception and design: M.A. Alfaqih, E.R. Nelson, R. Safi, E. Macias, M.R. Freeman, C.-y. Chang, D.P. McDonnell, S.J. Freedland
Development of methodology: M.A. Alfaqih, E.R. Nelson, W. Liu, J. Geradts, J.W. Thompson, M.R. Freeman, S.J. Freedland
Acquisition of data (provided animals, acquired and managed patients, provided facilities, etc.): M.A. Alfaqih, E.R. Nelson, R. Safi, E. Macias, J. Geradts, J.W. Thompson, L.G. Dubois, C.-y. Chang, S.J. Freedland
Analysis and interpretation of data (e.g., statistical analysis, biostatistics, computational analysis): M.A. Alfaqih, E.R. Nelson, W. Liu, R. Safi, J.S. Jasper, E. Macias, J. Geradts, L.G. Dubois, M.R. Freeman, C.-y. Chang, D.P. McDonnell, S.J. Freedland
Writing, review, and/or revision of the manuscript: M.A. Alfaqih, E.R. Nelson, W. Liu, R. Safi, J.S. Jasper, E. Macias, J. Geradts, J.W. Thompson, L.G. Dubois, M.R. Freeman, C.-y. Chang, J.-T. Chi, D.P. McDonnell, S.J. Freedland
Administrative, technical, or material support (i.e., reporting or organizing data, constructing databases): J.-T. Chi, D.P. McDonnell, S.J. Freedland
Study supervision: E. Macias, J.-T. Chi, D.P. McDonnell, S.J. Freedland

References

1. Siegel RL, Miller KD, Jemal A. Cancer statistics, 2016. CA Cancer J Clin 2016;66:7–30.
2. Platz EA, Clinton SK, Giovannucci E. Association between plasma cholesterol and prostate cancer in the PSA era. Int J Cancer 2008;123:1693–8.
3. Magura L, Blanchard R, Hope B, Beal JR, Schwartz GG, Sahmoun AE. Hypercholesterolemia and prostate cancer: A hospital-based case-control study. Cancer Causes Control 2008;19:1259–66.
4. Mondul AM, Weinstein SJ, Virtamo J, Albanes D. Serum total and HDL cholesterol and risk of prostate cancer. Cancer Causes Control 2011;22:1545–52.
5. Platz EA, Till C, Goodman PJ, Parnes HL, Figg WD, Albanes D, et al. Men with low serum cholesterol have a lower risk of high-grade prostate cancer in the placebo arm of the prostate cancer prevention trial. Cancer Epidemiol Biomarkers Prev 2009;18:2807–13.
6. Kok DE, van Roermund JG, Aben KK, den Heijer M, Swinkels DW, Kampman E, et al. Blood lipid levels and prostate cancer risk; a cohort study. Prostate Cancer Prostatic Dis 2011;14:340–5.
7. Schaffner CP. Prostatic cholesterol metabolism: Regulation and alteration. Prog Clin Biol Res 1981;279–324.
8. White CP. On the occurrence of crystals in tumours. J Pathol Bacteriol 1909;13:3–10.
9. Montero J, Morales A, Llacuna L, Lluis JM, Terrones O, Basañez G, et al. Mitochondrial cholesterol contributes to chemotherapy resistance in hepatocellular carcinoma. Cancer Res 2008;68:5246–56.
10. Mostaghel EA. Steroid hormone synthetic pathways in prostate cancer. Transl Androl Urol 2013;2:212–27.
11. Ukomadu C, Dutta A. Inhibition of cdk2 activating phosphorylation by mevastatin. J Biol Chem 2003;278:4840–6.
12. Mo H, Elson CE. Studies of the isoprenoid-mediated inhibition of mevalonate synthesis applied to cancer chemotherapy and chemoprevention. Exp Biol Med (Maywood, NJ) 2004;229:567–85.
13. Hamilton RJ, Banez LL, Aronson WJ, Terris MK, Platz EA, Kane CJ, et al. Statin medication use and the risk of biochemical recurrence after radical prostatectomy: Results from the Shared Equal Access Regional Cancer Hospital (SEARCH) Database. Cancer 2010;116:3389–98.
14. Oh DS, Song H, Freedland SJ, Gerber L, Patel P, Lewis S, et al. Statin use and prostate cancer recurrence in men treated with brachytherapy. ASTRO National Meeting 2011.
15. Mucci LA, Stampfer MJ. Mounting evidence for prediagnostic use of statins in reducing risk of lethal prostate cancer. J Clin Oncol 2014;32:1–2.
16. Geybels MS, Wright JL, Holt SK, Kolb S, Feng Z, Stanford JL. Statin use in relation to prostate cancer outcomes in a population-based patient cohort study. Prostate 2013;73:1214–22.
17. Nielsen SF, Nordestgaard BG, Bojesen SE. Statin use and reduced cancer-related mortality. N Engl J Med 2012;367:1792–802.
18. Yu O, Eberg M, Benayoun S, Aprikian A, Batist G, Suissa S, et al. Use of statins and the risk of death in patients with prostate cancer. J Clin Oncol 2014;32:5–11.
19. YuPeng L, YuXue Z, PengFei L, Cheng C, YaShuang Z, DaPeng L, et al. Cholesterol levels in blood and the risk of prostate cancer: A meta-analysis of 14 prospective studies. Cancer Epidemiol Biomarkers Prev 2015;24:1086–93.
20. Agalliu I, Salinas CA, Hansten PD, Ostrander EA, Stanford JL. Statin use and risk of prostate cancer: Results from a population-based epidemiologic study. Am J Epidemiol 2008;168:250–60.
21. Coogan PF, Kelly JP, Strom BL, Rosenberg L. Statin and NSAID use and prostate cancer risk. Pharmacoepidemiol Drug Saf 2010;19:752–5.
22. Chang CC, Ho SC, Chiu HF, Yang CY. Statins increase the risk of prostate cancer: A population-based case-control study. Prostate 2011;71:1818–24.
23. Haukka J, Sankila R, Klaukka T, Lonnqvist J, Niskanen L, Tanskanen A, et al. Incidence of cancer and statin usage–record linkage study. Int J Cancer 2010;126:279–84.
24. Brown MS, Goldstein JL. The SREBP pathway: Regulation of cholesterol metabolism by proteolysis of a membrane-bound transcription factor. Cell 1997;89:331–40.
25. Zelcer N, Tontonoz P. Liver X receptors as integrators of metabolic and inflammatory signaling. J Clin Invest 2006;116:607–14.
26. Hong C, Tontonoz P. Coordination of inflammation and metabolism by PPAR and LXR nuclear receptors. Curr Opin Genet Dev 2008;18:461–7.
27. Lee BH, Taylor MG, Robinet P, Smith JD, Schweitzer J, Sehayek E, et al. Dysregulation of cholesterol homeostasis in human prostate cancer through loss of ABCA1. Cancer Res 2013;73:1211–8.
28. Pommier AJ, Alves G, Viennois E, Bernard S, Communal Y, Sion B, et al. Liver X receptor activation downregulates AKT survival signaling in lipid rafts and induces apoptosis of prostate cancer cells. Oncogene 2010;29:2712–23.
29. Zhuang L, Kim J, Adam RM, Solomon KR, Freeman MR. Cholesterol targeting alters lipid raft composition and cell survival in prostate cancer cells and xenografts. J Clin Invest 2005;115:959–68.
30. Cali JJ, Russell DW. Characterization of human sterol 27-hydroxylase. A mitochondrial cytochrome P-450 that catalyzes multiple oxidation reaction in bile acid biosynthesis. J Biol Chem 1991;266:7774–8.
31. Radhakrishnan A, Ikeda Y, Kwon HJ, Brown MS, Goldstein JL. Sterol-regulated transport of SREBPs from endoplasmic reticulum to Golgi: Oxysterols block transport by binding to Insig. Proc Natl Acad Sci 2007;104:6511–8.
32. Sood AK, Saxena R, Groth J, Desouki MM, Cheewakriangkrai C, Rodabaugh KJ, et al. Expression characteristics of prostate-derived Ets factor support a role in breast and prostate cancer progression. Hum Pathol 2007;38:1628–38.
33. Norris JD, Chang CY, Wittmann BM, Kunder RS, Cui H, Fan D, et al. The homeodomain protein HOXB13 regulates the cellular response to androgens. Mol Cell 2009;36:405–16.
34. Nelson ER, Wardell SE, Jasper JS, Park S, Suchindran S, Howe MK, et al. 27-Hydroxycholesterol links hypercholesterolemia and breast cancer pathophysiology. Science (New York, NY) 2013;342:1094–8.
35. Shatnawi A, Tran T, Ratnam M. R5020 and RU486 act as progesterone receptor agonists to enhance Sp1/Sp4-dependent gene transcription by an indirect mechanism. Mol Endocrinol 2007;21:635–50.
36. Fritz LC, Diaz JL, Armstrong RC, Tomaselli KJ. Rapid methods for identifying modifiers of cellular apoptosis activity. 2001.
37. Heinlein CA, Chang C. Androgen receptor in prostate cancer. Endocr Rev 2004;25:276–308.
38. Yamamoto Y, Loriot Y, Beraldi E, Zhang F, Wyatt AW, Nakouzi NA, et al. Generation 2.5 antisense oligonucleotides targeting the androgen receptor and its splice variants suppress enzalutamide-resistant prostate cancer cell growth. Clin Cancer Res 2015;21:1675–87.
39. Sawada N, Sakaki T, Ohta M, Inouye K. Metabolism of vitamin D (3) by human CYP27A1. Biochem Biophys Res Commun 2000;273:977–84.
40. Li Y, Chan SC, Brand LJ, Hwang TH, Silverstein KAT, Dehm SM. Androgen receptor splice variants mediate enzalutamide resistance in castration-resistant prostate cancer cell lines. Cancer Res 2013;73:483–89.

41. Antonarakis ES, Lu C, Wang H, Luber B, Nakazawa M, Roeser JC, et al. AR-V7 and resistance to enzalutamide and abiraterone in prostate cancer. N Engl J Med 2014;371:1028–38.

42. Sato R, Inoue J, Kawabe Y, Kodama T, Takano T, Maeda M. Sterol-dependent transcriptional regulation of sterol regulatory element-binding protein-2. J Biol Chem 1996;271:26461–4.

43. Brown MS, Goldstein JL. A proteolytic pathway that controls the cholesterol content of membranes, cells, and blood. Proc Natl Acad Sci 1999;96:11041–8.

44. Yang J, Sato R, Goldstein JL, Brown MS. Sterol-resistant transcription in CHO cells caused by gene rearrangement that truncates SREBP-2. Genes Dev 1994;8:1910–9.

45. Chen Y, Hughes-Fulford M. Human prostate cancer cells lack feedback regulation of low-density lipoprotein receptor and its regulator, SREBP2. Int J Cancer 2001;91:41–5.

46. Leon CG, Locke JA, Adomat HH, Etinger SL, Twiddy AL, Neumann RD, et al. Alterations in cholesterol regulation contribute to the production of intratumoral androgens during progression to castration-resistant prostate cancer in a mouse xenograft model. Prostate 2010;70:390–400.

47. Murtola TJ, Syvala H, Pennanen P, Blauer M, Solakivi T, Ylikomi T, et al. The importance of LDL and cholesterol metabolism for prostate epithelial cell growth. PLoS One 2012;7:e39445.

48. Bjarnadottir O, Romero Q, Bendahl P-O, Jirström K, Rydén L, Loman N, et al. Targeting HMG-CoA reductase with statins in a window-of-opportunity breast cancer trial. Breast Cancer Res Treat 2013;138:499–508.

49. Alfaqih MA, Allott EH, Hamilton RJ, Freeman MR, Freedland SJ. Statins and prostate cancer prevention: Are we there yet? Nat Rev Urol 2017;14:107–19.

50. Singh P, Saxena R, Srinivas G, Pande G, Chattopadhyay A. Cholesterol biosynthesis and homeostasis in regulation of the cell cycle. PLoS ONE 2013;8:e58833.

51. Umetani M, Domoto H, Gormley AK, Yuhanna IS, Cummins CL, Javitt NB, et al. 27-Hydroxycholesterol is an endogenous SERM that inhibits the cardiovascular effects of estrogen. Nat Med 2007;13:1185–92.

52. Yeh CR, Da J, Song W, Fazili A, Yeh S. Estrogen receptors in prostate development and cancer. Am J Clin Exp Urol 2014;2:161–8.

53. Nelson AW, Tilley WD, Neal DE, Carroll JS. Estrogen receptor beta in prostate cancer: Friend or foe? Endocr Relat Cancer 2014;21:T219–34.

54. Raza S, Meyer M, Schommer J, Hammer KDP, Guo B, Ghribi O. 27-Hydroxycholesterol stimulates cell proliferation and resistance to docetaxel-induced apoptosis in prostate epithelial cells. Med Oncol 2016;33:1–9.

55. Fu W, Yao J, Huang Y, Li Q, Li W, Chen Z, et al. LXR agonist regulates the carcinogenesis of PCa via the SOCS3 pathway. Cell Physiol Biochem 2014;33:195–204.

56. Pencheva N, Buss Colin G, Posada J, Merghoub T, Tavazoie Sohail F. Broad-spectrum therapeutic suppression of metastatic melanoma through nuclear hormone receptor activation. Cell 2014;156:986–1001.

57. Li X, Chen Y-T, Hu P, Huang W-C. Fatostatin displays high antitumor activity in prostate cancer by blocking SREBP-regulated metabolic pathways and androgen receptor signaling. Mol Cancer Ther 2014;13:855–66.

58. Liang Y, Mafuvadze B, Aebi JD, Hyder SM. Cholesterol biosynthesis inhibitor RO 48-8071 suppresses growth of hormone-dependent and castration-resistant prostate cancer cells. Onco Targets Ther 2016;9:3223–32.

AUTHOR QUERIES

AUTHOR PLEASE ANSWER ALL QUERIES

Q1: Page: 1: AU: Per journal style, genes, alleles, loci, and oncogenes are italicized; proteins are roman. Please check throughout to see that the words are styled correctly. AACR journals have developed explicit instructions about reporting results from experiments involving the use of animal models as well as the use of approved gene and protein nomenclature at their first mention in the manuscript. Please review the instructions at http://www.aacrjournals.org/site/InstrAuthors/ifora.xhtml#genenomen to ensure that your article is in compliance. If your article is not in compliance, please make the appropriate changes in your proof.

Q2: Page: 1: Author: Please verify the drug names and their dosages used in the article.

Q3: Page: 1: Author: Please verify the affiliations and their corresponding author links.

Q4: Page: 1: Author: Please verify the corresponding author details.

Q5: Page: 1: Author: Note that AACR journals do not use such abbreviations as "BC" for "breast cancer," "CRC" for colorectal cancer, or "Pca" for "prostate cancer," or other *ad hoc* two-word abbreviations for diseases that incorporate a part of the body. However, these abbreviations are acceptable in tables or figures where space is an issue as long as they are defined in the legend or table notes.

Q6: Page: 2: Author: Units of measurement have been changed here and elsewhere in the text from "M" to "mol/L," and related units, such as "mmol/L" and "μmol/L," in figures, legends, and tables in accordance with journal style, derived from the Council of Science Editors Manual for Authors, Editors, and Publishers and the Système international d'unités. Please note if these changes are not acceptable or appropriate in this instance.

Q7: Page: 4: Author: Please verify the layout of Table 1 for correctness.

Q8: Page: 5: Author: Please confirm quality/labeling of all images included within this article. Thank you.

Q9: Page: 5: Author: Please define "PCa."

Q10: Page: 10: AU:/PE: The conflict-of-interest disclosure statement that appears in the proof incorporates the information from forms completed and signed off on by each individual author. No factual changes can be made to disclosure information at the proof stage. However, typographical errors or misspelling of author names should be noted on the proof and will be corrected before publication. Please note if any such errors need to be corrected. Is the disclosure statement correct?

Q11: Page: 10: Author: The contribution(s) of each author are listed in the proof under the heading "Authors' Contributions." These contributions are derived from forms completed and signed off on by each individual author. As the corresponding author, you are permitted to make changes to your own contributions. However, because all authors submit their contributions individually, you are not permitted to make changes in the

contributions listed for any other authors. If you feel strongly that an error is being made, then you may ask the author or authors in question to contact us about making the changes. Please note, however, that the manuscript would be held from further processing until this issue is resolved.

Q12: Page: 11: Author: Please verify the headings "Acknowledgments" and "Grant Support" and their content for correctness.

Q13: Page: 11: Author: Please provide journal name, volume, and page range for ref. 36.

AU: Below is a summary of the name segmentation for the authors according to our records. The First Name and the Surname data will be provided to PubMed when the article is indexed for searching. Please check each name carefully and verify that the First Name and Surname are correct. If a name is not segmented correctly, please write the correct First Name and Surname on this page and return it with your proofs. If no changes are made to this list, we will assume that the names are segmented correctly, and the names will be indexed as is by PubMed and other indexing services.

First Name	Surname
Mahmoud A.	Alfaqih
Erik R.	Nelson
Wen	Liu
Rachid	Safi
Jeffery S.	Jasper
Everardo	Macias
Joseph	Geradts
J. Will	Thompson
Laura G.	Dubois
Michael R.	Freeman
Ching-yi	Chang
Jen-Tsan	Chi
Donald P.	McDonnell
Stephen J.	Freedland